CHAPTER 5

INVESTIGATING SNARE-INTERACTIONS BY FUNCTIONAL COMPLEMENTATION IN *Saccharomyces cerevisiae* AND PULL-DOWN ASSAYS WITH α-SNAP

5.1. INTRODUCTION

In 1977 it was shown that a gene from a higher eukaryote could be expressed in a microorganism, *Escherichia coli*, to produce a biologically active protein, somatostatin (Kingsman *et al.* 1985). It appears, however, that *E. coli* may not be the most suitable host for the expression of all eukaryotic proteins. A disadvantage of the *E. coli* system is the necessity to renature the heterologous polypeptides, since in most cases this organism was found to be unable to produce the proteins in a properly folded, soluble form (i.e. not in inclusion bodies). Moreover, many eukaryotic proteins depend on post-translational modifications such as glycosylation, which prokaryotic hosts are unable to synthesize (Gellissen *et al.* 1992). In many instances yeast became the preferred hosts for heterologous protein and gene expression. The best-characterized species, *Saccharomyces cerevisiae*, was the first to be used for the successful production of eukaryotic proteins such as human α-interferon, hepatitis B surface antigens and enzymes like calf pro-chymosin and *Aspergillus* glucoamylase (Gellissen *et al.* 1992). Furthermore, the availability of the entire genome sequence of *S. cerevisiae*, as well as the *S. cerevisiae* genome deletion project, enables researchers to perform functional complementation in yeast.

5.1.1. *S. cerevisiae*: A model organism for studying protein transport

A basic feature of all eukaryotic cells is compartmental organization, which requires mechanisms for the correct sorting and distribution of molecules to the appropriate target organelle. Due to an impressive conservation of the molecular transport machinery across phyla (Rothman 1996), a great deal of knowledge on the functional interactions has been acquired by the study of *S. cerevisiae*. This yeast is a unicellular eukaryote, organized into the same major membrane-bounded compartments as all other eukaryotic cells and shares the same metabolic processes (Kucharczyk and Rytka 2001).

In *S. cerevisiae* delivery of cargo to the recipient organelle is accomplished by membrane recognition processes known as tethering, docking and fusion, similar to those described in mammalian cells. Tethering factors are peripherally membrane-associated protein complexes, containing up to 10 different subunits. The docking stage involves two specific sets of membrane-anchored SNARE proteins. Firstly the family of v-SNAREs (or synaptobrevin-related receptors) on the vesicle membranes and secondly, the t-SNAREs (or plasma membrane syntaxin related receptors) on the target membrane. The formation of a stable four-helical bundle between the v- and t-SNAREs is believed to generate enough energy to initiate mixing of the lipid bilayers of the fusing membranes (Sutton *et al.* 1998). In yeast, the proteins Sec18p and Sec17p, which are required at all transport steps, regulate complex formation. ATP hydrolysis by Sec18p disassembles the complex, similar to NSF in higher eukaryotic cells. In yeast, similar to mammalian cells, SNARE binding has been proven to be promiscuous and that multi-protein complexes determine the specificity of membrane fusion (Kucharczyk and Rytka 2001). The various interactions between v- and t-SNAREs in yeast are summarized in Figure 5.1. Apart from the functional similarities between yeast SNAREs and those of higher eukaryotes, the remarkable structural similarities have also been well described (Rossi *et al.* 1997; Katz and Brennwald 2000; Antonin *et al.* 2002; Fasshauer 2003).

Apart from the homologous SNAREs in yeast, the small monomeric Rab GTPases (200-230 amino acids) found in higher eukaryotic cells also occur in yeast i.e. the Ypt GTPases. These small Ypt GTPases belong to the Ras-related protein superfamily and play key regulatory roles at the different stages of trafficking. In *S. cerevisiae* this superfamily contains 29 members of which eleven are Ypt GTPases. Other families belonging to this superfamily include Ras that has a regulatory role in the cell cycle, Ran which regulates nuclear import, Arf/Sar which functions during vesicle budding and Rho, which regulates cytoskeletal organization and cell wall biogenesis (Kucharczyk and Rytka 2001).

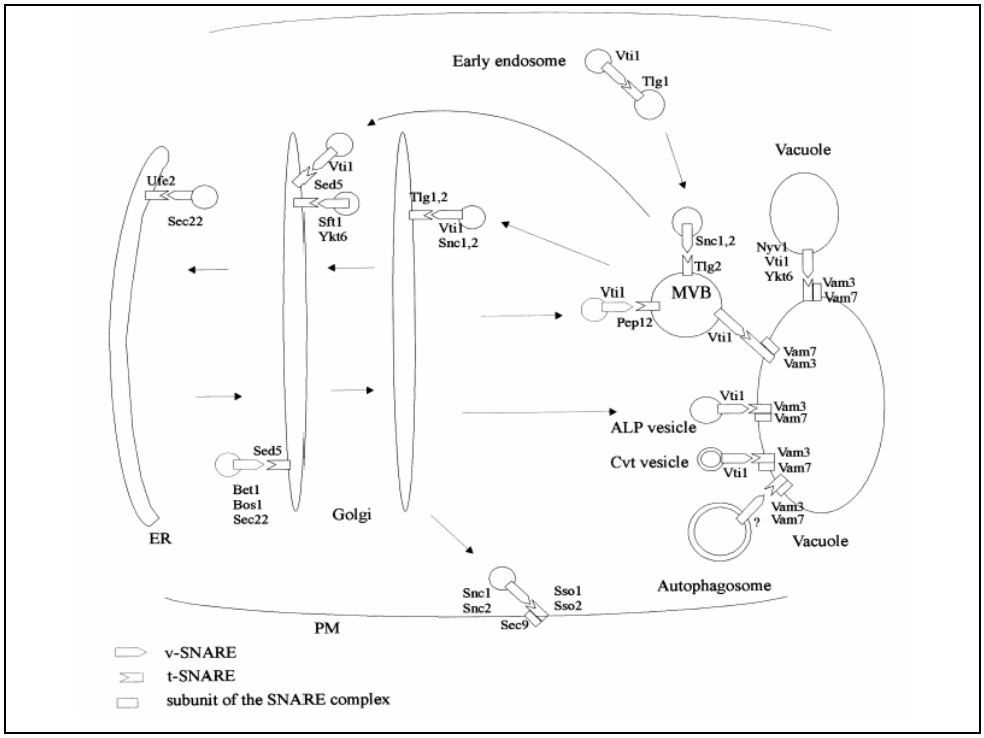

Figure 5.1. Interactions of v- and t-SNAREs in yeast (Kucharczyk and Rytka 2001). *Compartment abbreviations: (ER) endoplasmic reticulum, (PM) plasma membrane and (MVB) multivesicular body. The various yeast v- and t-SNAREs are indicated.*

Similar to higher eukaryotic GTPases, the transport GTPases in yeast also cycle between active GTP-bound and inactive GDP-bound conformations. Furthermore, the cycle is regulated in an identical manner as in mammalian cells by means of GDP-dissociation inhibitors (GDI), GDI displacement factors (GDF) and GTPase-activating proteins (GAP), as described in Chapter 2 (Kucharczyk and Rytka 2001). A high degree of conserved sequence motifs occur between Ras proteins from different species (Table 5.1), enabling functional complementation studies.

Table 5.1. Conserved sequence motifs in Ras proteins from different species (Kucharczyk and Rytka 2001). *G1 binds α and β phosphates of GTP/GDP; G2 is the effector domain essential for GTP hydrolysis; G3 binds γ phosphate of GTP; G4 binds the guanine ring; G5 stabilizes the guanine-G4 interaction.*

	G1	G2	G3	G4	G5
Ypt7 (Yeast)	GDSGVGKT	YKATI	WDTAGQE	GNKID	FL-TSAK
p21 / ras (Rat)	GAGGVGKS	YDPTI	LDTAGQE	GNKCD	FIETSAK
RhoH (Human)	GDGGCGKT	YTPTV	WDTAGQD	GCKTD	YHRGQEM
Ran (Mouse)	GDGGTGKT	YVATL	WDTAGQE	GNKVD	YYDISAR

Apart from the conserved proteins involved in trafficking, yeast also exhibits signal regulation of the various trafficking steps, i.e. clathrin, Vps34p phosphatidylinositol 3-kinase and the Vps15 protein kinase which has been indicated to regulate the formation of Golgi vesicles, which carry cargo to the multi vesicular body (Conibear and Stevens 1995). It is proposed that Vps15p and Vps34p function together as components of a membrane-associated signal transduction complex that regulates intracellular protein trafficking through protein and lipid phosphorylation (Kucharczyk and Rytka 2001).

The lipid constituents of the plasma membrane, i.e. phosphatidylinositols (PI), sphingolipids and sterols are not only present in *S. cerevisiae*, but have also been proven to be important transport regulators, similar to higher eukaryotic cells (Kucharczyk and Rytka 2001). This confirms that in all eukaryotes, not only proteins, but also lipids play a vital role in trafficking. PIs, which are substrates for various PI kinases and PI phosphatases have been studied extensively. In *S. cerevisiae*, it has been shown that PI-4,5-P_2 plays a role in internalization of clathrin-mediated endocytosis and that PI-3-P functions at a post-internalization step of endocytosis as well as endosomal/vacuolar trafficking. Spingolipids and ergosterol form sterol-sphingolipid-rich domains (rafts) in the plasma membrane. These rafts are believed to define the membrane spatial specificity by recruiting the endocytic machinery to a distinct membrane site and also delivery of some proteins to the plasma membrane (Kucharczyk and Rytka 2001).

Other multi cellular processes linked to transport and trafficking, including actin cytoskeletal dynamics and ubiquitylation, have also been studied extensively in yeast and were shown to resemble processes in higher eukaryotes (Shaw *et al.* 2001).

5.1.2. Functional complementation

Functional complementation involves the controlled expression of a heterologous (e.g. non-yeast) proteins in mutated or knockout cells (e.g. yeast cells) in order to rescue a particular phenotype.

Yeast vectors used for heterologous protein expression

Five common types of plasmids are used for yeast transformation. Vectors of the YIp type (yeast integration plasmid) integrates by homologous recombination of complementation genes contained on the plasmid at the respective mutant loci of suitable auxotrophic

acceptor strains. Integrative transformants are extremely stable and therefore often used as production strains containing or producing a heterologous protein. Vectors of the YRp type (yeast replication plasmid) remain in an extra-chromosomal state after transformation due to the presence of a sequence for autonomous replication (*ARS*). They are present in 3-20 copies, but are very unstable due to abnormal segregation during mitosis or meiosis. The plasmid stability was improved with the addition of a yeast centromeric sequence, leading to the YCp (yeast centromeric plasmid) vectors. Addition of telomeric structures in YAC (yeast artificial chromosomes) lead to linear vectors that can harbour DNA fragments up to 200 kb in size. The most commonly used vectors in yeast engineering are derived from the 2 μm plasmid, termed YEp (yeast episomal plasmid) vectors. They can transform yeast at a frequency of 5 000 – 20 000 recombinants per μg of DNA and transformants contain an average of 40 copies per cell and also exhibit high stability (Gellissen *et al.* 1992). For expression, a heterologous gene is fused to a promoter obtained from a highly expressed *S. cerevisiae* gene (see Chapter 4) as well as a yeast derived termination sequence.

In this study we investigated the use of the pRS 413 plasmid, which is an autonomously replicating single copy centromeric (YCp) plasmid (http://www.atcc.org/Products/prs.cfm). It is also an *S. cerevisiae* / *E. coli* shuttle vector which allows ampicillin and blue/white selection in *E. coli* (lacZ). It contains the ADH-promoter and termination fragments, as well as a HIS3 selection marker in *S. cerevisiae* (Figure 5.2).

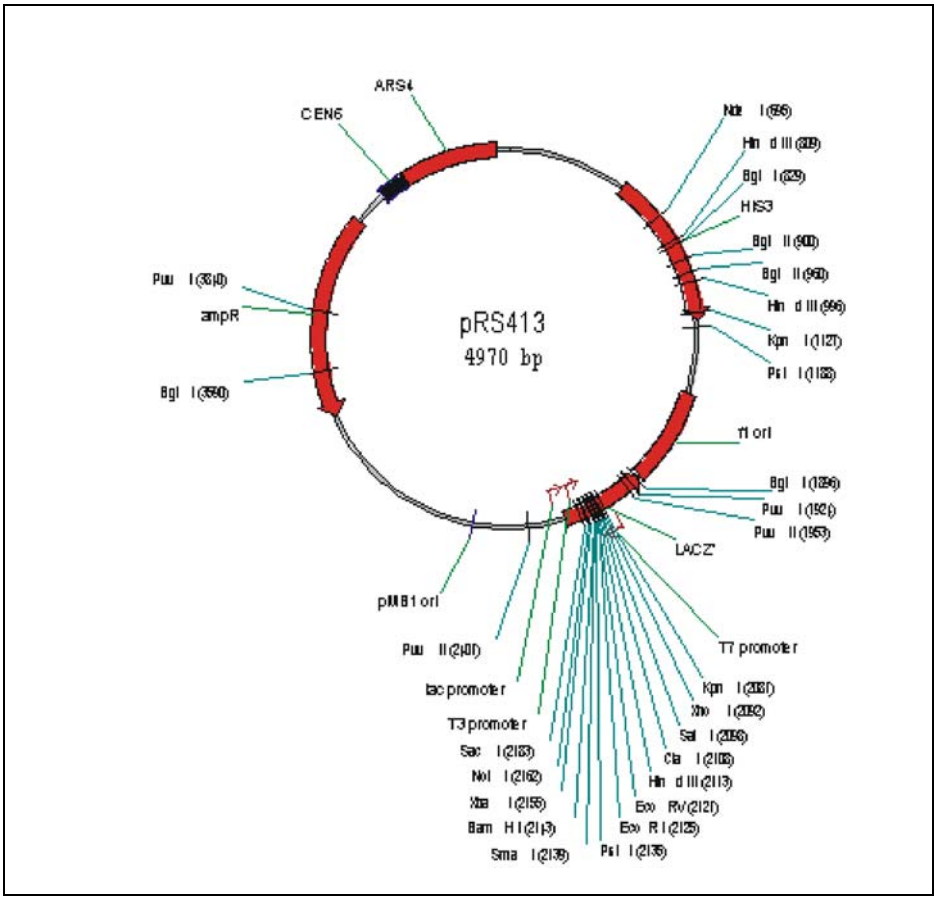

Figure 5.2. Plasmid map of the *S. cerevisiae* / *E. coli* shuttle vector pRS 413 (Clontech Laboratories 1997a).

Subcellular localization of heterologous proteins

It has been shown that the presence or absence of a 'classical' signal sequence on a heterologous protein does not necessarily determine the subcellular localization in *S. cerevisiae* (Kingsman *et al.* 1985). For example, the proteins preprochymosin, prochymosin and chymosin have all been expressed in *S. cerevisiae,* and all forms located to the cell membrane and none in the cytoplasm. Similar results were obtained during the expression of hepatitis B surface antigen, which lacks a signal sequence. Expression of these constructs in a yeast strain with the *pep4-3* mutation (which is deficient in vacuolar proteases) increased the yields, indicating that proteolytic degradation of foreign proteins occurs (Kingsman *et al.* 1985).

Glycosylation

Evidence for the glycosylation of heterologous proteins in *S. cerevisiae* comes from studies on α_1-antitrypsin and mouse immunoglobulins. Expression of the latter yielded high

molecular weight forms which were not present in tunicamysin-treated cultures or after endoglycosidase H or chemical de-glycosylation (Kingsman *et al.* 1985). It must be noted that the percentage of glycosylation is low and heterogeneous. Also, *S. cerevisiae* glycoproteins are of the high-mannose type, whereas higher eukaryotic glycoproteins contain a variety of glycosyl residues with complex branching. It is therefore unlikely that glycosylation of heterologous proteins in *S. cerevisiae* will contribute to any biological activity, which requires complex and specific carbohydrate modifications (Kingsman *et al.* 1985).

5.1.3. Functional complementation of SNAREs and trafficking proteins in yeast

In spite of all the obstacles, functional complementation of both *SSO-1* and *SSO-2* (yeast syntaxin) as well as a *pep12* (homologue of yeast and mammalian syntaxins) mutants were successful. In the case of the temperature-sensitive mutations in the yeast syntaxin 1, homologous Sso1p and Sso2p, a screen for high copy number suppressors of the phenotype yielded three genes from a genomic yeast library that are involved in the terminal step of secretion: *SNC1*, *SNC2* (synaptobrevin homologues) and *SEC9* (a SNAP25 homologue) (Jantti *et al.* 2002).

The yeast protein pep12 is a syntaxin homologue, which may function in the trafficking of vesicles from the trans-Golgi network to the vacuole. By means of functional complementation of the yeast pep12 mutant with an *Arabidopsis thaliana* cDNA library, a pep12 homologue was identified. The *Arabidopsis* cDNA encodes a 31 kDa protein which is homologous to yeast pep12 and other members of the syntaxin family (Bassham *et al.* 1995). The existence of plant homologues of syntaxins indicates firstly, that the basic vesicle docking and fusion machinery may be conserved in plants as it is in yeast and mammals and secondly, that cross-species expression and functional complementation of syntaxin homologues are feasible in yeast.

In another functional complementation study using *S. cerevisiae* and an *Arabidopsis thaliana* cDNA library, a homologue that complements the *sec14* mutant was identified. AtSEC14 was able to restore the growth of sec14 temperature sensitive mutants, partly restored protein secretion and enhanced the phosphatidylinositol-transfer activity that is impaired in *sec14* mutants. Interestingly, the best sequence similarity between yeast sec14 and AtSec14 is

found at the amino acid level (36.5% similar) and not the genomic level (Jouannic *et al.* 1998). Our results obtained by the two-hybrid assay (Chapter 4) are similar to the latter.

Transport between secretory pathways also requires SNAREs. By means of functional complementation in *YKT6* knockout yeast (which encodes a novel SNARE involved in ER to Golgi transport), three SNAREs, p14, p28 and p26 were identified from human cDNA libraries. These proteins were found to be homologous to their yeast counterparts, Sft1p, Gos1p and Ykt6p. Important to note is that the SNARE, Ykt6p, which requires membrane localization for protein function, still localized to the membrane in yeast without the isoprenylation signal. Furthermore, this study demonstrated that Ykt6p and its homologues are highly conserved between yeast and human and it is the first example of a human SNARE protein functionally replacing a yeast SNARE. This observation implies that the specific details of the vesicle targeting code, like the genetic code, are conserved in evolution (McNew *et al.* 1997).

In a study by Pullikuth *et al.* the *in vivo* role of the insect NSF (MsNSF), isolated from the insect *Manduca sexta* (the so-called tabacco hormworm) was investigated by heterologous expression in *SEC18* mutated yeast. *M. sexta* MsNSF is believed to regulate hormone release from the endocrine/paracrine cells of the corpora allata. MsNSF was shown to be functional in yeast membrane fusion *in vivo* and rectified defects in the mutated yeast at nearly all discernable steps where Sec18p has been implicated in the biosynthetic route (Pullikuth and Gill 2002).

5.1.4. α-SNAP: Functional properties

It has long been known that *in vitro* α-SNAP binds directly to syntaxin and SNAP25, but not to VAMP (McMahon and Sudhof 1995). Upon formation of a α-SNAP-syntaxin complex, VAMP can be bound. In the presence of all three SNAREs as well as NSF, pull-down assays using immobilized α-SNAP results in the purification of all three SNAREs and NSF. This indicates that syntaxin, VAMP and SNAP25 are SNAP receptors (Hanson *et al.* 1995; McMahon and Sudhof 1995).

Despite limited overall sequence similarity among SNAREs on different membranes, all SNARE complexes examined to date bind α-SNAP and can be disassembled by NSF (Marz *et al.* 2003). All SNARE complexes contain four SNARE helices, are rod-shaped and held

together by interactions among conserved, mostly hydrophobic residues, within the core of the complex. Crystal structures of both the neuronal and endosomal SNARE complexes indicated that these complexes have largely acidic surface potentials, but contain few conserved residues on the outer solvent-exposed surfaces (Antonin *et al.* 2002; Marz *et al.* 2003).

To date, little is known about how α-SNAP recognizes the variety of SNARE complexes. By means of deletion studies in bovine α-SNAP and structural modeling of the data on the Sec17p (yeast α-SNAP homologue) crystal structure, Marz *et al.* were able to show that shape complementarity, sequence conservation and overall surface charge distribution are important factors for protein interactions (Marz *et al.* 2003).

The model proposed for α-SNAP binding to SNARE complexes shows that α-SNAP binds SNAREs in an anti-parralel orientation, positioning the N-terminal near the membrane and the C-terminal away from the membrane where it interacts with NSF. By mutating basic residues, SNARE binding was reduced up to 20% indicating that charged α-SNAP residues (which are distributed over the concave surface) are involved in the binding of SNARE complexes (Figure 5.3).

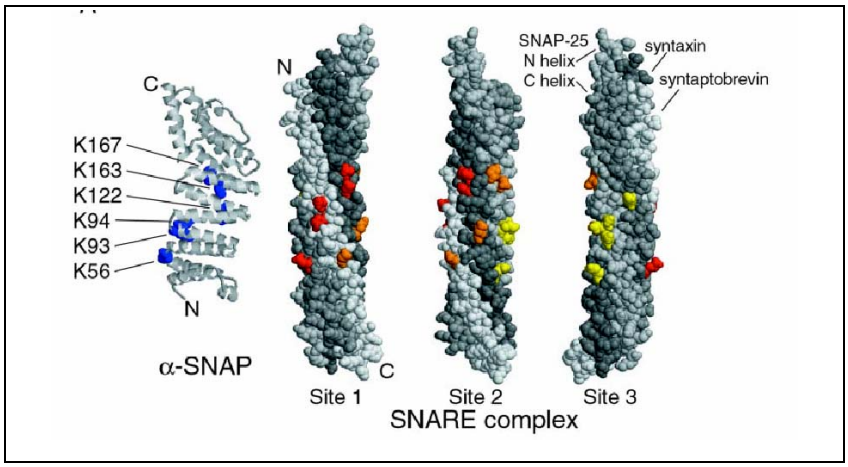

Figure 5.3. Putative α-SNAP binding sites on the SNARE complex (Marz *et al.* 2003). *Left, ribbon diagram of α-SNAP homology model, showing basic residues (blue) whose mutation reduces SNARE complex binding. Right, conserved acidic residues on the SNARE complex define three potential binding sites for α-SNAP. These sites are designated Site 1 (red, syntaxin Asp-214, Asp-218; synaptobrevin Asp-51, Glu-55; SNAP-25 C-terminal helix Glu-183), Site 2 (orange, SNAP-25 N-terminal helix Glu-38, Asp-41; syntaxin Glu-228; synaptobrevin Asp-65), and Site 3 (yellow, SNAP-25 C-terminal helix Asp-166; SNAP-25 N-terminal helix Asp-51, Glu-52, Glu-55; syntaxin Glu-238).*

Previous studies indicated that each 20S complex consists of one SNARE complex, three α-SNAPs and one NSF hexamer (Marz *et al.* 2003). The model created by Marz *et al.* indicated that the basic residues of α-SNAP form a diagonal band across the face of the α-SNAP sheet domain and that this band pairs with a diagonal band of acidic residues on the SNARE complex (Marz *et al.* 2003). Pairing of the charged diagonal bands allowed the authors to align three α-SNAP twisted sheet domains with a single SNARE complex (Figure 5.4). In this arrangement, shape complementarity is maximized and is substantially greater than when SNAPs are placed directly parallel to individual SNARE helixes. This may explain why α-SNAP binding to individual SNAREs is weaker than to the SNARE complex and why α-SNAP dissociates after complex disassembly.

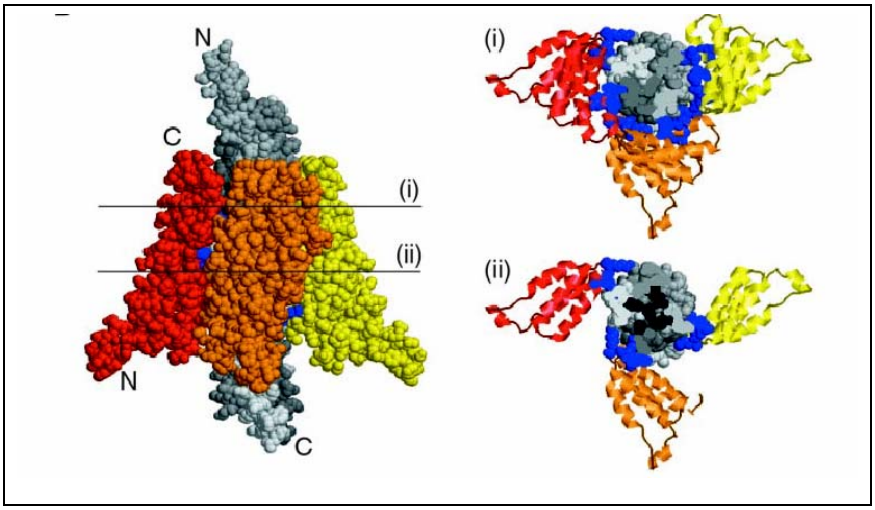

Figure 5.4. Proposed SNAP-SNARE binding model (Marz *et al.* 2003). *Indicated are the three α-SNAP twisted sheet domains bound to the SNARE complex. Each α-SNAP is color-coded according to the SNARE complex site to which it binds. Lines through the model show where slices were made to generate axial views (i) and (ii). Views are from the N-terminal and cytoplasmic ends of the SNARE complex. Basic residues whose mutations reduce SNARE complex binding, are colored blue. The SNARE complex ionic layer is colored black.*

Taking into account all of the above listed properties of α-SNAP, we decided on exploiting recombinant rat brain α-SNAP in order to isolate all of its binding partners from the salivary glands of *O. savignyi* by means of affinity chromatography (pull-down assays).

5.2. HYPOTHESIS

- We hypothesize that the SNARE proteins and α-SNAP of *O. savignyi* share both structural and functional similarity to the SNAREs of other eukaryotic cells, such as yeast and rat brain.

5.3. AIMS

- Functional complementation of the syntaxin 1 homology SSO-1 and SSO-2 mutated yeast strains using an *O. savignyi* salivary gland cDNA library.
- Expression of rat brain α-SNAP.
- Isolation of α-SNAP binding proteins from *O. savignyi* salivary glands using affinity chromatography (pull-down assays) with immobilized recombinant rat brain α-SNAP.

5.4. MATERIALS

The SSO1 and SSO2 mutated yeast strains H603 and H902 were obtained from Dr. Jussi Jantti of the VTT Technical Research Centre of Finland, VTT Biotechnology, Finland and Prof. Hans Ronne from the Department of Plant Biology, Swedish University of Agricultural Sciences, Sweden. Yeast expression plasmids were a kind gift from Prof. Carol Sibley, Department of Genetics, University of Washington, Seattle, USA. The Super SMART™ cDNA synthesis kit was obtained from Clontech (Southern Cross Biotechnology). KC8 *E. coli* cells were a kind gift from Dr. Hannelie Moolman-Smook, University of Stellenbosh, South Africa. Recombinant α-SNAP was a kind gift from Proff. Whiteheart and Rothman at the Memorial Sloan-Kettering Cancer Institute, New York, USA. NucleoSpin® Plasmid Quick Pure, NucleoBond® PC2000, NucleoSpin® Extract kits and Protino® Ni 150 columns were from Macherey-Nagel, Germany (Separations). PCR nucleotide mix (10 mM deoxynucleotide solution), *Sfi* I restriction enzyme and Shrimp alkaline phosphatase were from Roche Diagnostics. Peptone, agar and yeast nitrogen base without amino acids were from Difco (Labretoria). Yeast extract and tryptone were purchased from Oxoid Ltd. (England). Deoxyribonucleic acid sodium salt type III from salmon testes, 3-amino-1,2,4-triazole (3-AT), cycloheximide, , RNase Inhibitor, PEG4000, 425-600 micron glass beads, Triton X-100 and all the various amino acids used were from Sigma. Dextrose, Isopropyl β-D-thiogalactopyranoside (IPTG), 5-bromo-4-chloro-3-indolyl-β-D-galactopyranoside (X-gal), L-adenine hemisulphate, lithium acetate, ammonium acetate and ampicillin were from ICN (Separations). DNA polymerase I large (Klenow) fragment, *Taq* Polymerase, *Pfu* DNA polymerase, Proteinase K and various restriction enzymes were from Promega (Wisconsin, USA). BugBuster™ was from Novagen, USA. TaKaRa Ex Taq (5 U/μl) and T4 DNA Ligase (350 U/μl) were from Takara Bio Inc., Japan (Separations). All primers were synthesized by Inqaba Biotech (Pretoria, South Africa). Anti-IgG (whole molecule) conjugated to peroxidase was from Cappel (Separations). The GelCode® SilverSNAP™ stain kit was from Pierce, USA (Separations).

5.5. METHODS

5.5.1. *O. savignyi* salivary gland cDNA library construction

cDNA libraries were constructed using the Super SMART™ system, as described previously (Chapter 3 and 4). In order to directionally clone the inserts into the pRS413 vector, various restriction enzyme recognition sequences were incorporated into the CDS and SMART primers, respectively. The properties of the primers are listed in Table 5.2.

5.5.2. Growth and maintenance of *SSO*-mutated yeast cells

The SSO1 and SSO2 mutated yeast exhibit a temperature-sensitive phenotype. Therefore, cells from both H603 and H902 strains were grown at 24ºC in a shaking incubator in adenine supplemented YPD media (YPDA, 20 g/l peptone, 10 g/l yeast extract, 20 g/l agar, 20g/l dextrose, 0,03g/l adenine hemisulphate). In order to obtain sufficient cells for library transformation, cells were grown for 4 - 6 days.

5.5.3. Transformation, selection and screening

Large-scale yeast transformation was performed as described in Chapter 4. Following transformation, cells were plated on SD/-His and incubated at 30ºC in order to identify positive transformants with a suppressed phenotype. Clones were screened using nested PCR (see Chapter 4) and unique clones were selected and grown at 30ºC in SD/-His at 30ºC, in a shaking incubator. Plasmid isolation from the positive yeast clones was done as decribed in Chapter 4 and transformed into *E. coli* cells in order to obtain sufficient plasmid for DNA sequencing.

5.5.4. Data analysis

Sequences obtained were analyzed using the BioEdit Program. DNA and deduced protein sequences were analyzed using BLAST-P, PSI-BLAST (www.ncbi.nlm.nih.gov/BLAST) and the threading program 3D-PSSM Web Server V 2.6.0 (www.igb.uci.edu/tools/scratch/). All alignments were performed with Clustal W (www.ebi.ac.uk/clustalw/).

5.5.5. Expression of rat brain α-SNAP

Rat brain α-SNAP (cloned into the pQE-9 vector) was transformed into BL21 *E. coli* cells. Colonies selected from ampicillin-agar plates were grown for 12 hours at 30ºC in 5 ml LB-Broth containing 1:1 000 ampicillin. Four milliliters of culture were diluted into 50 ml LB-Broth and incubated at 30ºC in a shaking incubator until A_{660} ~ 0.6. Isopropryl-β-D-thiogalactopyranoside was added to a final concentration of 2.5 mM and cultures incubated for another 3 hours. The cells were collected by centrifugation (10 000 x g, 10 min) and aspirated, before determining the wet weight of the pellet. Cells were completely resuspended in 5 ml BugBuster™ per gram of wet cell paste containing 10 μg/ml DNAse, 1 μg/ml leupeptin, 20 μg/ml aprotonin and 0.5 mM PMSF (phenylmethylsulfonyl fluoride). Cells were incubated on a rotating mixer at 8ºC overnight. Insoluble debris was removed by

centrifugation (13 000 x g, 20 min, 4ºC) and the supernatant transferred to a fresh tube. The supernatant was loaded directly onto a Ni-column or stored at –70ºC until needed.

5.5.6. Salivary gland homogenate preparation

Salivary glands (~20 glands) were dissected from female, unfed *O. savignyi* ticks. Glands were suspended in homogenization buffer (20 mM HEPES pH 7.4, 100 mM KCl, 5 mM ATP, 1 mM mercapto-ethanol, 0,5% Triton X100) containing 1 μg/ml Leupeptin, 20 μg/ml aprotonin and 0.5 mM PMSF and incubated overnight at 8ºC on a rotating platform. Insoluble debris was removed by centrifugation (13 000 x g, 20 minutes, 4ºC) and the supernatant was used immediately for affinity chromatography or stored at –70ºC.

5.5.7. Affinity chromatography (Pull-down assays)

Polyhistidine-tagged recombinant α-SNAP was isolated using the Protino® Ni 150 pre-packed columns from Macherey-Nagel. Columns were equilibrated in 320 μl LEW buffer (50 mM NaH_2PO_4, 300 mM NaCl, pH 8.0) and the cell lysate, prepared with BugBuster™, was loaded and allowed to elute with gravity. Columns were washed once with 320 μl of LEW before loading the clarified salivary gland homogenates. Non-specific bound proteins were removed by washing the column two times with 320 μl LEW. Specifically bound protein was eluted with 800 μl elution buffer (50 mM NaH_2PO_4, 300 mM NaCl, 250 mM imidazole, pH 8.0).

5.5.8. ELISA

Samples obtained after affinity chromatography were distributed into a 96 well microtiter plate (50 μl /well), dried under a 150 W lamp in a stream of air generated by an electric fan, and subsequently blocked with 300 μl of TBS (pH 7.4) containing 0.5% casein for 60 minutes. Blocking medium was replaced with 50 μl of primary antibody containing medium (diluted 1:1 000 in blocking buffer) and incubated at 37ºC for 60 minutes. Plates were washed three times in blocking buffer and incubated with an appropriate anti-IgG (whole molecule) peroxidase conjugate at a 1:10 000 dilution. After a second washing step, 100 μl developing buffer (10 ml citrate, 10 mg OPD and 8 mg H_2O_2, pH 4.5) was added and the reaction monitored at 450 nm.

5.5.9. SDS-PAGE

Samples obtained after affinity chromatography were dialyzed against 20 mM Tris-HCl (pH 8) overnight at 8ºC with stirring and freeze dried prior to SDS-PAGE. SDS-PAGE was performed

using a 5% stacking gel (0.625 M Tris-HCl, 0.5% SDS, pH 6.8) and 12% separating gel (1.88 M Tris-HCl, 0.5% SDS, pH 8.8). The acrylamide gels and the electrophoresis buffer were prepared from an acrylamide stock (30% acrylamide, 0.8% N',N'-methylene bisacrylamide) and electrophoresis buffer stock (0.02M Tris-HCl, 0.06% SDS, 0.1 M glycine, pH 8.3). The gel solutions were polymerized with the addition of 30 μl of 10% ammonium persulphate and 5 μl TEMED. Samples were resuspended in reducing sample buffer (0.06 M Tris-HCl, 2% SDS, 0.1% glycerol, 0.05% β-mercaptoethanol, 0.025% bromophenol blue) and boiled at 95ºC for 5 minutes. Pre-stained molecular mass markers (Pierce, USA) were dissolved in 10 μl water. Electrophoresis was carried out in a Biometra electrophoresis system (Biometra GmbH, Germany) with an initial voltage of 60 V for 45 minutes and thereafter a voltage of 100 V until the bromophenol blue marker reached the bottom of the gel. Gels were stained using the GelCode® SilverSNAP™ stain from Pierce.

5.6. RESULTS AND DISCUSSION

5.6.1. cDNA library construction

Although a cDNA library constructed in the two-hybrid plasmid (pACT2) was available for performing functional complementation studies in the SSO-mutant yeast, we decided to create a new cDNA library that does not contain the DNA-AD domain. In order to clone the inserts directionally, SMART and CDS primers containing *Bam*HI and *Eco*RI sites were designed and used for cDNA and ds DNA construction using the SMART system as described previously. The properties of the primers are listed in Table 5.2.

Table 5.2. Properties of the primers used for SMART cDNA synthesis of the *Bam*H I/*Eco*R I library.

Name	Sequence	Tm (°C)
*Bam*H I SMART	AAG CAG TGG TAT CAA CGC AGA GTC GGA TCC GGG G *Bam*H I	74.3
*Eco*R I CDS	AAG CAG TGG TAT CAA CGC AGA GTG AAT TC$(T)_{18}$ VN *Eco*R I	67.3

During amplification of the cDNA, a smear ranging from 200 to 2000 bp were obtained (Figure 5.5.i). This is identical to the results described previously (Chapters 3 and 4). After digestion with *Bam*HI and *Eco*RI, the library was digested to such an extent that it was regarded as inadequate for cloning (Figure 5.5.ii). This indicates that there are multiple digestion/recognition sites for *Bam*HI and *Eco*RI in the ds cDNA of *O. savignyi* salivary glands.

Based on the list of frequency of restriction enzyme cutters from BioLabs, (http://www.neb.com/neb/tech/tech_resource/restriction/properties), we designed a new SMART primer which contains a low frequency *Sac* I restriction site. As a CDS primer, we used the CDSIII primer which is decribed in Chapters 3 and 4. This primer contains not only an *Sfi* I site, but also *Xba* I and *Nco* I sites. The properties of the primers are listed in Table 5.3.

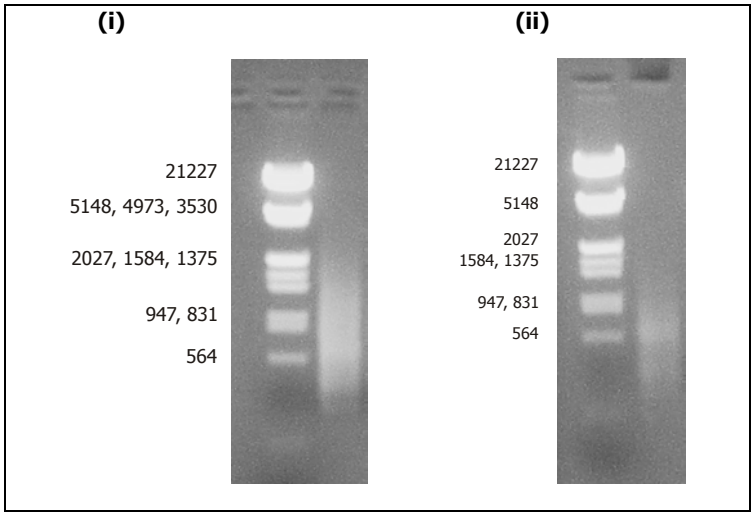

Figure 5.5. Agarose gel electrophoresis of (i) the ds SMART cDNA synthesized using the *Bam*H I SMART- and *Eco*R I CDS primers and (ii) the SMART ds DNA after *Bam*H I and *Eco*R I digestion.

Table 5.3. Properties of the primers used for SMART cDNA synthesis of the *Sac* I/*Xba* I library.

Name	Sequence	Tm (°C)
Sac I SMART	AAG CAG TGG TAT CAA CGC AGA GTC GAG CTC GGG G *Sac* I	74.3
CDS III / 3'PCR	5' ATT CTA GA**G GCC TCC ATG GCC** GAC ATG $(T)_{30}$NN 3' *Xba* I **Sfi I** *Nco* I	67.3

After cDNA synthesis and LD-PCR amplification we obtained a smear ranging between 200 and 2000 bp (Figure 5.6). Following digestion of the library with *Sac* I and *Xba* I (which is present on the pRS 413 plasmid), the library was completely digested into very small fragments (i.e. *Sac* I and *Xba* I are frequent cutters) and again not regarded as useful for cloning. In order to clone the salivary gland cDNA library, one would need to incorporate a suitable rare cutter restriction enzyme site for *O. savignyi* (such as *Sfi* I) into the pRS413 plasmid, since it does not contain a suitable restriction site. Prior to altering the plasmid, we decided to exploit the possibility of using the full-length *Sfi* I two-hybrid fusion library for the functional complementation studies. Based on the findings in literature that fusion constructs, such as GFP tagged proteins, do not interfere with SNARE binding, localization or function, we decided on using the two-hybrid full-length *Sfi* I cDNA library cloned into the pACT2 vector.

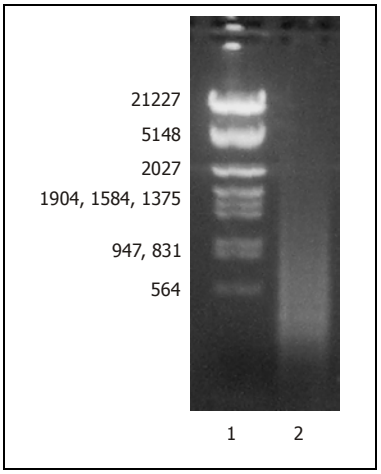

Figure 5.6. Agarose gel electrophoresis of the ds SMART cDNA synthesized using the *Sac* I SMART- and CDS III primer. *Lane 1 corresponds to the molecular mass standards, and lane 2 to the cDNA library obtained after 24 cycles using the Sac I SMART- and CDS III primers.*

5.6.2. Growth and maintenance of syntaxin knockout yeast

During the study of Jäntti *et al.*, various *SSO1* and *SSO2* mutants were generated (Jantti *et al.* 2002). They were able to show that Sso1p is essential for sporulation, while Sso2p is important for protein secretion. Only two strains were used during this functional complementation study, i.e. H603 and H902 that both contain deletions of the *SSO1* gene and contain a mutated *SSO2* gene. The properties of the two strains are listed in Table 5.4. The strains differ in their origin, i.e. H603 is derived from the W303 strain while H902 is derived from the NY179 strain, which contribute the various markers (Table 5.4). Therefore, by performing complementation in both strains, the W303 and NY179 background effects can be investigated. Cells were grown in a shaking incubator in YPDA medium at 24ºC.

Table 5.4. Properties of the SSO-mutated temperature sensitive yeast strains

Name	Genotype	Markers
H603	a, *sso*1-Δ1::*HIS3 sso*2-1	*ade2-1*, *can 1-100*, *his3-11*, *15leu2-3*, *112 trp1-1 ura3-1*
H902	a, *sso*1-Δ1::*LEU2 sso*2-1	*leu2-3*, *112*, *ura3-52*

5.6.3. Transformation, selection and screening

Mutated H603 cells were transformed with the pACT2 full-length *Sfi* I salivary gland cDNA library from fully engorged, female *O. savignyi* salivary glands using the 30x library scale TRAFCO transformation protocol (Chapter 4). Positive H603 transformants were selected on SD/-Leu/-His plates and grown at 37ºC to select inserts that suppress the temperature

sensitive phenotype. Nested PCR directly from positive clones were performed using the pACT2-nested primers (Chapter 4). Restriction enzyme mapping (*Bam*HI and *Hind*III) of some 40 clones identified four unique inserts (Figure 5.7). These were isolated and transformed into KC8 *E. coli* cells in order to obtain sufficient plasmid for DNA sequencing. Restriction enzyme mapping of the inserts from KC8 cells confirmed the presence of four unique clones (Figure 5.8), which were isolated and sequenced.

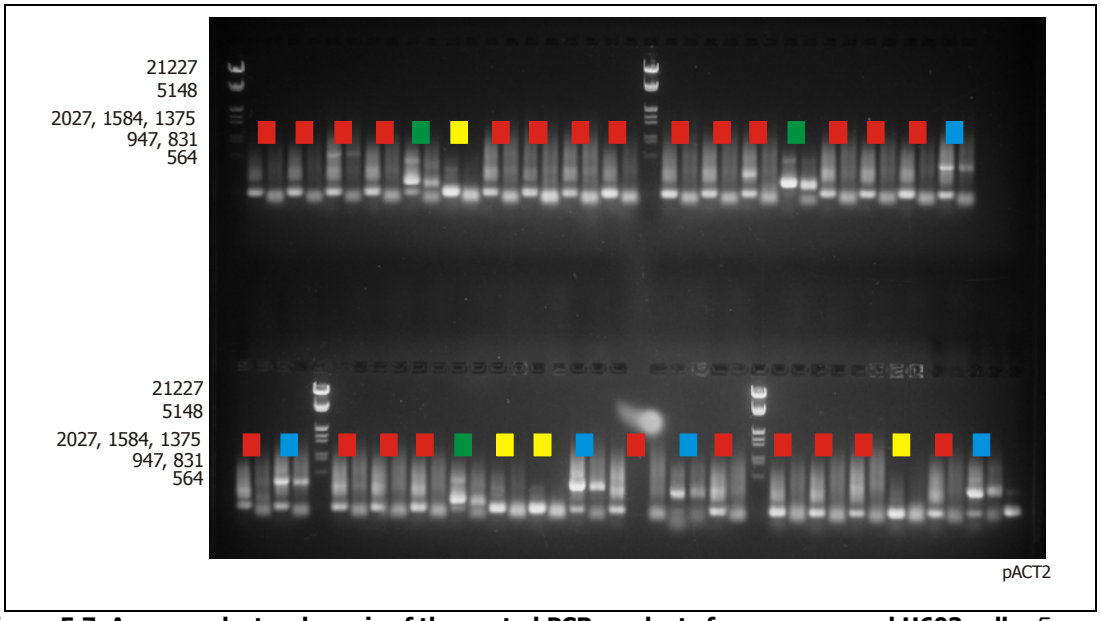

Figure 5.7. Agarose electrophoresis of the nested PCR products from suppressed H603 cells. *For each clone the undigested as well as the BamH I/Hind III digested inserts are shown. Unique inserts (coloured blocks) are indicated.*

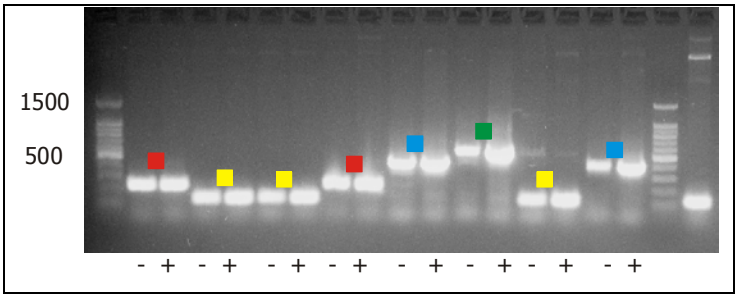

Figure 5.8. Agarose electrophoresis of the nested PCR products from KC8 cells.
Undigested (-) BamH I and Hind III digested (+) and unique inserts (coloured blocks) are shown.

5.6.4. Data analysis

The deduced amino acid sequences of the four unique inserts were determined and are listed in Table 5.5. These correspond to 30, 81, 135 and 91 amino acid peptides for clone 5, 20, 23 and 27, respectively. The peptides were further analyzed by multiple sequence alignment of the syntaxin family (obtained from Pfam) using Clustal X. By aligning the peptide sequences with the syntaxin family sequences (Figure 5.9) and calculating the similarity and identity between various sequences, we were able to show that clones 20, 23 and 27 share homology with syntaxins sso2 from yeast, syntaxin 7 from human and syntaxin from fungi, respectively (Table 5.6).

Sequence comparisons between various mammalian full-length syntaxins indicated that they share 27-44% similarity (Advani *et al.* 1998). When non-mammalian syntaxins are included, the similarity is reduced to 30-35%. Since the calculated values (given in Table 5.6) are representative of the identified protein fragment (domain) vs. the full-length syntaxins, the calculated values are decreased, but still significant (see Figure 5.10 and 5.11).

Table 5.5. Deduced amino acid sequence of inserts that suppressed the SSO1 temperature sensitive phenotype of H603 cells.

Name	Amino acid sequence
Clone 5	AGHVTRSLTVKLNKWQQRKKKXKKKKKKHV
Clone 20	WSHGPVKVAADAVRGQYSELLEAGSLPHQPKQRVLGLSRVYIRCTCAPCTASTKEKKPGVDVLRCKYLRNGALNKCGSCQA
Clone 23	WGLHPNMVLKCPEITDKDKIYKTLPQPSCIYYCGQEEESGRYKYGFLRDNSTCKLAPTLNGYCYKGHCYKYPGGQQVTTTTEA GVTEKSTGRPSQTRRPSPTRRPSPTRRPSPTKKTKATKKPSDQKKKKKKKKN
Clone 27	GQQADCRNSRAFEKTERRRGAKKAGGRSQNQGRRRSGAFEARETEARARTQREEETERKGKEKLHLQRKLRSQRRKKKKKKK

Table 5.6. Calculated similarities and identities between identified protein domains and various full-length syntaxin isoforms. *The encoded protein sequence of the knockout clones that suppressed the temperature sensitive phenotype, was compared to that of various known syntaxins (column 1) of various organism. The similarity and identity between the isolated fragment (domain) and the full-length syntaxin was calculated using the BioEdit program.*

	Clone 20		**Clone 23**		**Clone 27**	
	% Identity	**% Similarity**	**% Identity**	**% Similarity**	**% Identity**	**% Similarity**
SSO2_Yeast/36-131	14	30	12	27	10	26
SSO1_Yeast/32-127	7	20	13	26	7	33
Q9P8G5/59-154 (Fungi)	14	24	16	27	17	35
Q9VU45/43-135 (Drosophila)	13	27	13	25	17	32
O70319/11-107 (Rat)	13	24	14	26	15	33
1Dn1_B/Syntaxin 1 (Human)	8	13	12	19	9	18
STX7_Human/7-101	16	27	16	29	19	34

Figure 5.9. Multiple sequence alignment of syntaxins and knockout suppressor peptides. *Non polar- (blue), negative charged- (purple), uncharged – (green), positive charged – (orange) and proline (yellow) residues are indicated. The three isolated peptides (H603 clones 20, 23 and 27) as well as a similarity scale are shown.*

Alignment of the peptide encoded by clone 20 with the human syntaxin 1 (1Dn1_B, used for modelling in Chapter 4) indicated the aligned regions of the sequences to share 23% identity and 38% similarity with the C-terminal domain (residues 237-273) of syntaxin 1 (Figure 5.10). Similarly, the peptide encoded by clone 27 shares 19% identity and 37% similarity to the aligned N-terminal domain (residues 27-83) of human syntaxin 1 (Figure 5.11). Clone 23 did not align to human syntaxin 1.

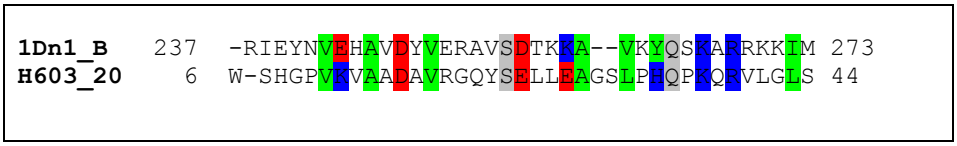

Figure 5.10. Multiple sequence alignments of clone 20 (H603_20) and human syntaxin 1 (1Dn1_B). *Non-polar (green), negative charged (red), positive charged (blue) and polar uncharged (grey) residues are indicated.*

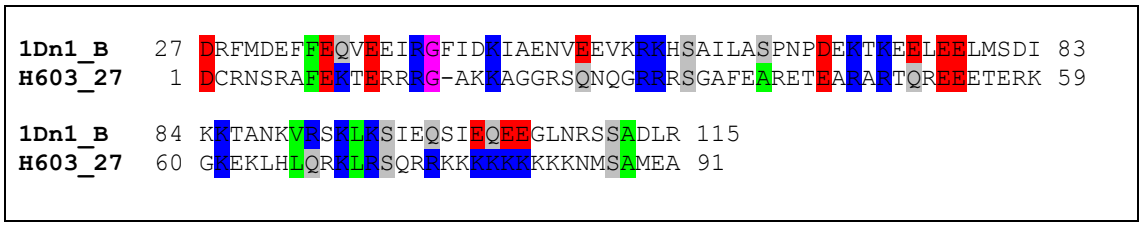

Figure 5.11 Multiple sequence alignments of clone 27 (H603_27) and human syntaxin 1 (1Dn1_B). *Non-polar (green), negative charged (red), positive charged (blue) and polar uncharged (grey) residues are indicated.*

Secondary structure prediction of the peptides indicated that clones 20 and 27, which align best with the syntaxins, are rich in alpha helical structure (Figure 5.12). Both clones 20 and 27 contain two α-helical domains while clone 23 only contains a short 9 residue C-terminal α-helix.

Threading analysis of clone 20 did not identify any significant similarities, but clone 23 was found to share 24% structural identity to the SH3 domain of human intersectin 2 (which acts as a scaffold during Clathrin mediated endocytosis). Clone 27 shares 29% structural identity to the complexin/SNARE complex, also known as the synaphin/SNARE complex (Figure 5.13). The latter complex contains the normal four-helix SNARE complex with complexin bound in an anti-parallel α-helical conformation in the groove between VAMP and syntaxin helices. Complexin is believed to stabilize the interface between the latter two helices, which bears the repulsive forces between the opposed membranes (Chen *et al.* 2002).

```
Clone 20:

WSHGPVKVAADAVRGQYSELLEAGSLPHQPKQRVLGLSRVYIRCTCAPCTASTKEKKPGV
...S.HHHHHHHHHHHHHHHHTT......T.EEEEEEEEEEEE.............TT.
eeeeeee---ee-eee-ee--eeeeeeeeeeee-ee--e---e-e-ee-eeeeeeeeeee

DVLRCKYLRNGALNKCGSCQA
.EEEHHHHHHHHHHTTS....
e--e-ee-eeeeeee-ee-ee

Clone 23:

WGLHPNMVLKCPEITDKDKIYKTLPQPSCIYYCGQEEESGRYKYGFLRDNSTCKLAPTLN
....TTEEEE......TTHEEEE.....EEEEE..EEETSEEEEEEEE.T...EE....T
eeeeee---e-ee-eeeee-eee-eeee-----eeeeeeee-e----eeeee-ee-ee-e

GYCYKGHCYKYPGGQQVTTTTEAGVTEKSTGRPSQTRRPSPTRRPSPTRRPSPTKKTKAT
EEEEETEEEE.TT..EEEEEEETTEEE...S.........................E..
-e--e-e--e-eeeee-eeeeeee-eeeeeeeeeeeeeeeeeeeeeeeeeeeeeeeeee

KKPSDQKKKKKKKKNV
....HHHHHHHHHT..
eeeeeeeeeeeeeee


Clone 27:

GQQADCRNSRAFEKTERRRGAKKAGGRSQNQGRRRSGAFEARETEARARTQREEETERKG
......T..HHHHHHHHHHT.HHTT.....TT....HHHHHHHHHHHHHH..HHHHHHHT
eeeee-eeeeeeeeeeeee-eeeeeeeeeeeeeeeeeeeeeeeeeeeeeeeeeeeeeee

KEKLHLQRKLRSQRRKKKKKKKKKNMSAMEA
HHHHHHHHHHHHHHHHHHHHHHHHHHHHHH..
eeeee-eeeeeeeeeeeeeeeeee-eeeee
```

Figure 5.12. Secondary structure prediction of the knockout suppressor peptides. *Line 1: The 1-letter code of the protein primary sequence. Line 2: 8-class secondary structure prediction (H: alpha helix, E: extended strand, T: turn, S: bend, G: 310-helix). Line 3: Prediction of relative solvent accessibility. Symbols corresponds to (-) the residue is buried, and (e) the residue is exposed.*

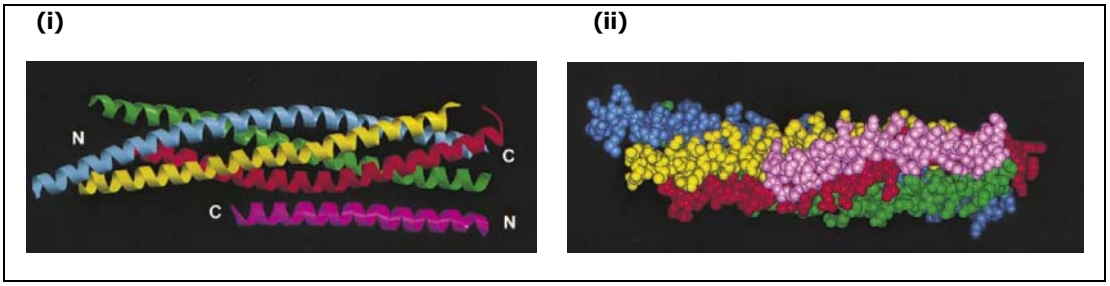

Figure 5.13. Structure of the Complexin / SNARE Complex (Chen *et al.* 2002). (i) Ribbon diagram with the following coloring code: yellow, syntaxin; red, synaptobrevin; blue, SNAP-25 N-terminal SNARE motif; green, SNAP-25 C-terminal SNARE motif; pink, complexin. (ii) Space filling model of the complexin/ SNARE complex.

Finally, we modeled the peptide encoded by clone 27 on the known crystal structure of syntaxin 1A using Modeller. From the model it is clear that the peptide share structural homology to the N-terminal domain of syntaxin 1A (Figure 5.14).

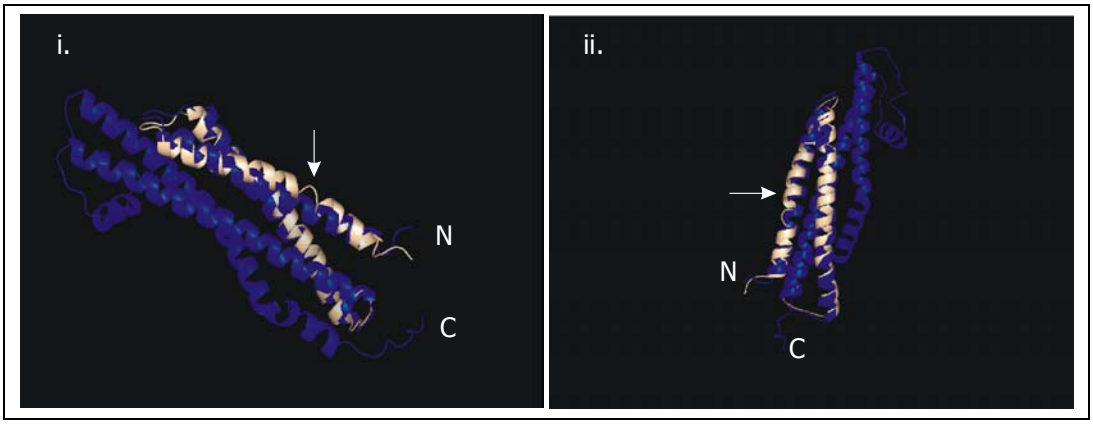

Figure 5.14. Modeled structure of the knockout fragment encoded by clone 27. *Superimposed model of the backbone structure of the knockout peptide from clone 27 (brown) on that of syntaxin 1A crystal structure (blue). The horizontal view (i), horizontal view (ii), N-terminal (N), C-termianl (C) and the single region for which no crystal data is available (arrow) is indicated. Structures were generated using Modeller and viewed using PyMol.*

In order to finally classify clone 20 and 27 as syntaxins, we need to obtain the full-length sequence of the encoded transcript and also investigate their effect on protein secretion from the H603 cells, as described by Jantti *et al*. (Jantti *et al.* 2002). To confirm that the suppressor effects are not due to the W303 cell background, these plasmids must be tested in H902 cells as well. The data obtained during this study is inconclusive in suggesting a possible identity for clone 23. Determining the entire open reading frame of the transcript is essential for identification. Regarding clone 5, no significant analysis could be performed due to the short length of the deduced peptide.

5.6.5. Pull-down assays

Isolation of the SNAREs from *O. savignyi* salivary glands were done by affinity chromatography, using immobilized recombinant rat brain α-SNAP and allowing salivary gland homogenates to bind. Eluates were investigated for the presence of SNAREs using ELISA and SDS-PAGE. ELISA with syntaxin, SNAP25, VAMP and Rab3a (negative control) polyclonal antibodies indicated signals 2.6 and 22.7 fold that of the negative control (Figure 5.15), confirming the presence of all three SNARE proteins in the eluate.

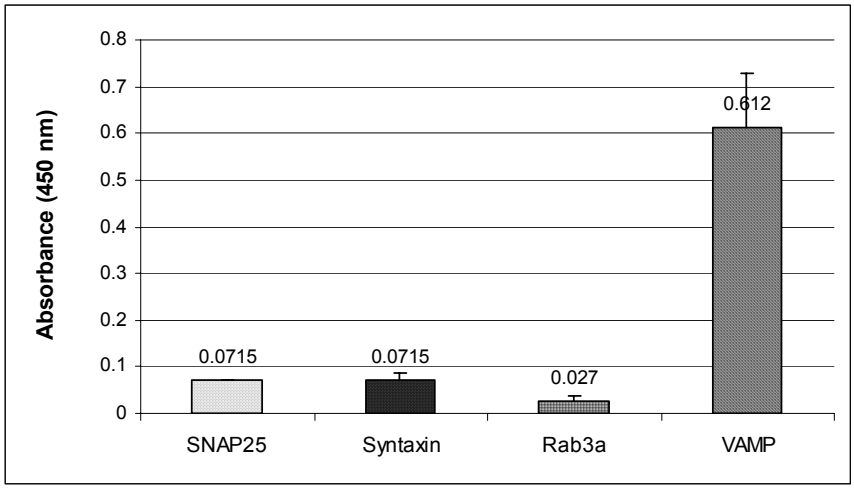

Figure 5.15. ELISA of pull-down eluates using polyclonal antibodies against the various SNAREs and Rab3a.

SDS-PAGE of the eluate confirmed the ELISA results. In the absence of salivary gland homogenates only recombinant α-SNAP is detected, but the three tick SNAREs (as determined by Western blotting, results not shown) are detected in samples obtained after performing the pull-down assay (Figure 5.16). The elevated level of VAMP is visible, explaining the high signal obtained during ELISA. In all cases, the migration rate of α-SNAP increased (lane 2), possibly due to proteolytic cleavage of α-SNAP by a protease present in the salivary gland homogenate. This must however be confirmed during future studies.

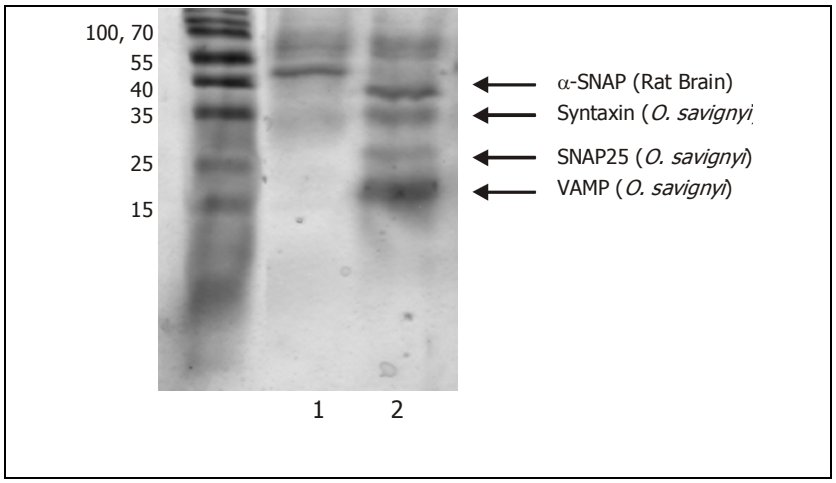

Figure 5.16. SDS-PAGE of pull-down eluates. *Lane 1 corresponds to recombinant α-SNAP isolated using the nickel column, while lane (2) corresponds to the eluate obtained after pull-down assays with O. savignyi salivary gland homogenates.*

Interestingly, very high amounts of VAMP were isolated compared with that of syntaxin and SNAP25. This can be explained from literature where it has been shown that the α-SNAP-syntaxin as well as the α-SNAP-syntaxin-SNAP25 complexes forms high affinity biding sites for VAMP (Hanson *et al.* 1995; McMahon and Sudhof 1995). Future studies will entail the protein sequencing of these SNAREs, amplification of their encoding transcripts and comparing their sequences to those of known SNAREs and those identified during functional complementation and two-hybrid studies.

5.7. CONCLUSION

During this study, functional complementation was used to successfully identify fragments of a putative syntaxin homologue from an *O. savignyi* salivary gland cDNA library. This *in vivo* system requires a functional protein domain in order to rescue the phenotype (temperature sensitive, secretion impaired), indicating that the identified domain is biologically capable of doing so. The syntaxin homologue identified differs from the syntaxin homologue that was identified using the two-hybrid system with α-SNAP as bait (Figure 5.17). The two domains share a similar charge distribution, but only 25% similarity and 13% identity to each other.

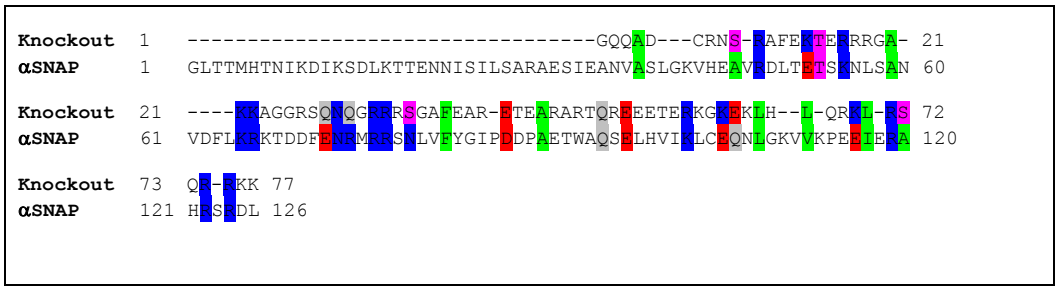

Figure 5.17. Multiple sequence alignment of the putative syntaxins isolated from *O. savignyi* salivary glands. *The sequence identified during functional complementation (Knockout) and two-hybrid screening using α-SNAP as bait (αSNAP) is shown. Non-polar (green), negative charged (red), positive charged (blue) and polar uncharged (gray) residues are indicated.*

Binding of syntaxin to α-SNAP is promiscuous and does not specifically relate to interactions occurring at the plasma membrane, while functional complementation requires biological activity in rescuing secretion at the plasma membrane of the yeast. It could therefore be that the two domains are representative of two different syntaxin isoforms. This must be further investigated by determining the entire coding regions of the domains and amino acid sequence comparison.

A novel feature of the knockout yeast used during this study is the possibility of investigating the effect of the various domains on protein secretion. These studies will be conducted during future investigations, in order to confirm their biological relevance.

By using affinity chromatography with α-SNAP we were able to identify the protein homologue of syntaxin, VAMP and SNAP25 from crude homogenates of *O. savignyi* salivary glands. These proteins share structural similarity to SNAREs found in rat brain, since they

cross-reacted with anti-rat brain SNARE antibodies. Amino acid sequencing of these will be indispensable for further cloning and investigations on the SNAREs of *O. savignyi*.

5.8. REFERENCES

Advani, R.J., Bae, H.R., Bock, J.B., Chao, D.S., Doung, Y.C., Prekeris, R., Yoo, J.S., Scheller, R.H. (1998). Seven novel mammalian SNARE proteins localize to distinct membrane compartments. *The Journal of Biological Chemistry* **273**(17): 10317-10324.

Antonin, W., Fasshauer, D., Becker, S., Jahn, R., Schneider, T.R. (2002). Crystal structure of the endosomal SNARE complex reveals common structural principles of all SNAREs. *Nature Structural Biology* **9**(2): 107-111.

Bassham, D., Gal, S., Conceicao, A., Raikhel, N.V. (1995). An *Arabidopsis* syntaxin homologue isolated by functional complementation of a yeast *pep12* mutant. *Proceedings of the National Academy of Science of the United States of America* **92**: 7262-7266.

Chen, X., Tomchick, D.R., Kovrigin, E., Arac, D., Machius, M., Sudhof, T.C., Rizo, J. (2002). Three-dimensional structure of the complexin/SNARE complex. *Neuron* **33**: 397-409.

Clontech Laboratories, I. (1997a). *Matchmaker Gal4 Two-hybrid vectors handbook (PT3062-1)*.

Conibear, E., Stevens, T.H. (1995). Vacuolar biogenesis in yeast: Sorting out the sorting proteins. *Cell* **83**: 513-516.

Fasshauer, D. (2003). Structural insights into the SNARE mechanism. *Biochimica et Biophysica Acta* **1641**: 87-97.

Gellissen, G., Melber, K., Janowicz, Z.A., Dahlems, U.M., Weydemann, U., Piontek, M., Strasse, A.W.M., Hollenberg, C.P. (1992). Heterologous protein production in yeast. *Antonie van Leeuwenhoek* **62**: 79-93.

Hanson, P.I., Otto, H., Barton, N., Jahn, R. (1995). The N-ethylmaleimide sensitive fusion protein and alpha-SNAP induce a conformational change in syntaxin. *The Journal of Biological Chemistry* **270**(28): 16955-16961.

Jantti, J., Aalto, M.K., Oyen, M., Sundqvist, L., Keranen, S., Ronne, H. (2002). Characterization of temperature-sensitive mutations in the yeast syntaxin 1 homologues Sso1p and Sso2p, and evidence of a distinct function for Sso1p in sporulation. *Journal of Cell Science* **115**: 409-420.

Jouannic, N., Lepetit, M., Vergnolle, C., Cantrel, C., Gardies, A.M., Kader, J.C., Arondel, V. (1998). Isolation of a cDNA from *Arabidopsis thaliana* that complements the sec14 mutant of yeast. *European Journal of Biochemistry* **258**: 402-410.

Katz, L., Brennwald (2000). Testing the 3Q:1R Rule: Mutational analysis of the ionic zero layer in the yeast exocytic SNARE complex reveals no requirement for arginine. *Molecular Biology of the Cell* **11**: 3849-3858.

Kingsman, S.M., Kingsman, A.J., Dobson, M.J., Mellor, J., Roberts, N.A. (1985). Heterologous gene expression in *Saccharomyces cerevisiae*. *Biotechnology and Genetic Engineering Reviews* **3**: 377-416.

Kucharczyk, R., Rytka, J. (2001). *Saccharomyces cerevisiae* - a model organism for the studies on vacuolar transport. *Acta Biochimica Polonica* **48**(4): 1025-1042.

Marz, K.E., Lauer, J.M., Hanson, P.I. (2003). Defining the SNARE complex binding of alpha-SNAP. *The Journal of Biological Chemistry* **278**(29): 27000-27008.

McMahon, H.T., Sudhof, T.C. (1995). Synaptic core complex of synaptobrevin, syntaxin and SNAP25 forms high affinity alpha-SNAP binding site. *The Journal of Biological Chemistry* **270**(5): 2213-2217.

McNew, J.A., Sogaard, M., Lampen, N.M., Machida, S., Ye, R.R., Lacomis, L., Tempst, P., Rothman, J.E., Sollner, T. (1997). Ykt6p, a prenylated SNARE essential for endoplasmic reticulum - Golgi transport. *The Journal of Biological Chemistry* **272**(28): 17776-17783.

Pullikuth, A.K., Gill, S.S. (2002). *In vivo* membrane trafficking role for an insect N-ethylmaleimide sensitive factor which is developmentally regulated in endocrine cells. *The Journal of Experimental Biology* **205**: 911-926.

Rossi, G., Saliminen, A., Rice, L.M., Brunger, A.T., Brennwald, P. (1997). Analysis of a yeast SNARE complex reveals remarkable similiarity to the neuronal SNARE complex and a novel function for the C terminus of the SNAP-25 homolog, Sec9. *The Journal of Biological Chemistry* **272**(26): 16610-16617.

Rothman, J.E. (1996). The protein machinery of vesicle budding and fusion. *Protein Science* **5**: 185-194.

Shaw, J.D., Cummings, K.B., Huyer, G., Michaelis, S., Wendland, B. (2001). Yeast as a model system for studying endocytosis. *Experimental Cell Research* **271**: 1-9.

Sutton, R.B., Fasshauer, D., Jahn, R., Brunger, A.T. (1998). Crystal structure of a SNARE complex involved in synaptic exocytosis at 2.4 A. *Nature* **395**: 347-353.